

# Study of Bio-Effects of Millimeter Wave Propagation on Tissue

Sujata Mendgudle\* and Manmohan S. Bhatia

**Abstract**—This paper highlights the effect of millimeter wave (MMW) radiation on biological tissue for prolonged exposure to record thermal effects. The novel method described in this article is simulation of exposure of millimeter waves on tissues and study the thermal effects resulting from radiation. To simulate this, a setup to uniformly irradiate a tissue of about 2.2 mm thickness is described, and 3D visualization of MMW propagation is modeled using COMSOL Multiphysics radio frequency module at frequencies around 30 GHz. Heat generation and consequent temperature rise in the three-layer tissue structure is followed by analysis of temperature variation due to radiation absorption.

## 1. INTRODUCTION

Millimeter waves have found important applications in bio-electromagnetic domain, such as treatment modalities using MMW radiation. Various applications like cancer treatment, water purification, material wave interaction, food irradiation, waste water treatment, etc. are possible. This article focuses on radiation effects on tissues and gives brief analysis of effect of millimeter wave on biological tissue. The model is designed in COMSOL Multiphysics radio frequency (RF) module with waveguide and horn antenna structure to generate a uniform exposure zone. The dimensions of the exposure tissue were drawn from the range of considerations related to radiation, absorption, and heat diffusion. The mode of propagation of millimeter wave through the rectangular waveguide bend is captured for various time delays. The output of rectangular waveguide bend is coupled to the horn antenna structure. The TE<sub>10</sub> mode is propagated through bent waveguide which has cutoff frequency of 30 GHz. The scattering parameter  $S_{11}$  is obtained from the simulation tool for the study of effect of millimeter wave on the tissue. For free space Boundary Element Method (BEM), numerical technique is used. The waveguide structure is simulated by finite element method (FEM) numerical technique. The propagation characteristics of millimeter-waves in the presence of the human body are studied in [1]. In this paper, four models of body and parts are considered to evaluate thermal effects of millimeter-wave radiation on it. Paper [1] concludes that an ideal power density is not useful to evaluate thermal effect of millimeter wave on human tissue. For safety-based compliances with human body, a novel temperature-based technique is proposed in [1]. It is very important to incorporate the material properties of skin while modeling the effect of millimeter waves, because skin is a multi-layered tissue. These skin properties are evaluated using FEM techniques to characterize the visco-elasticity in skin which correlates with diseases [2]. Also, the electrical and thermal properties of tissues play a vital role in the analysis of effect of millimeter wave [3]. The long-term exposure to millimeter waves on skin is the object of the study that we cover in this paper, especially the absorption to heat temperature rise at frequencies around 30 GHz. As stated in earlier work, specific absorption rate (SAR) is not sufficient to calculate the dosimeter reading, and a thermal route looks promising. Thus, it is necessary to do thermal modeling for investigation of effect of MMW on skin [4]. The tissue structure used in our model has an outer layer about 0.1 mm thickness

---

*Received 6 September 2019, Accepted 2 January 2020, Scheduled 21 January 2020*

\* Corresponding author: Sujata Mendgudle (mendgudle123@gmail.com).

The authors are with the Department of Electronics Engineering, Ramrao Adik Institute of Technology, Nerul, Navi Mumbai, (affiliated to Mumbai University), India.

with an inner layers of 2 mm and 0.1 mm thicknesses, respectively as shown Fig. 2, which has different water contents according to the thickness and hence different responses to mm waves. Considering skin effect, anisotropy of tissue sub-layers in terms of water content and presence of different tissue compositions poses a tough task which requires a Multiphysics approach and for this COMSOL results may show more accuracy. In the radio wave communication, the utilization of frequency band increases with respect to the next generation technology. In 5G technology, due to higher frequency, the new challenges of EMF exposure to human body arises [5]. The radiated power density from the 5G devices needs to be studied to evaluate its harmful effects on human body. Thus, the restriction of SAR limit on such devices is very important. SAR increases with increase in frequency and decrease in skin depth. Some details of absorption of millimeter wave in human body is given in [6]. Several potential problems arise from irradiation in the millimeter-wave band with and without clothing. The whole body consists of complex layers such as epidermis, dermis, fats, subcutaneous, muscle, and blood. These complex layers can be heated and injured by prolonged millimeter wave radiations [7]. It is necessary to have an understanding of microwave theory to model such a complex body structure and its effects [8]. The heating of water using microwave is modeled in [9]. Similar heat production at millimeter wave range and its basics are explained in [10].

This paper dealing with effects of MMW on tissues is organized in four sections. Section 1 details the simulation framework planned. The required mathematical equations are given in Section 2. The results of heat generation and temperature variation of tissue with respect to time at millimeter wave frequency are given in Section 3. Based on the mathematical models, the numerical model is developed, and its results are discussed in Section 4. This paper is concluded in Section 5. The block diagram of the entire system, in which the power transmitted through the mm wave source is coupled to isolator and waveguide and finally radiates via horn antenna is shown in Fig. 1 whereas tissue dimensions are shown Fig. 2.

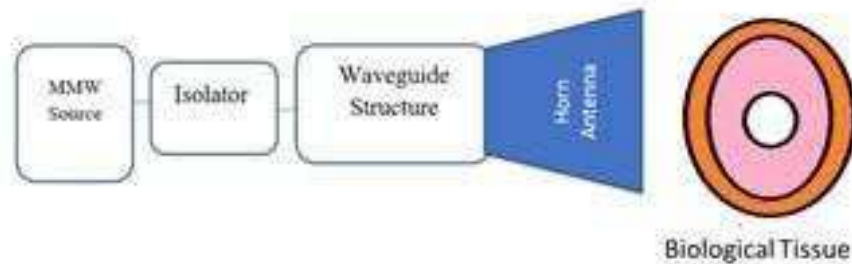


**Figure 1.** Block diagram of the proposed model.

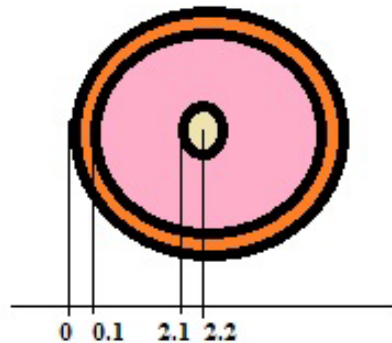


**Figure 2.** Tissue dimensions.

## 2. MATHEMATICAL MODELLING

This section gives the mathematical analysis of the entire model. The basic aim of this section is to calculate scattering parameters ( $S_{11}$ ) for the study of depth of penetration ( $\delta$ ). Actual 3D visualization of propagation of millimeter wave through waveguide bend is studied. Here, values of electrical and thermal properties of epidermis are considered from proven literature as follows, conductivity 39.18 S/m, relative permittivity 5.79, and depth of penetration 0.37 [7]. Similarly, mass density (Md) of tissue is 1100 kg/m<sup>3</sup>, and Applied Electric field,  $E = 5$  V/m, is considered. The mathematical model for the transverse  $E$ -field, which propagates through the waveguide at TE<sub>10</sub> mode, is necessary to calculate  $S$ -parameter. The power transmitted through the waveguide, which is coupled to horn antenna, creates uniform exposure on the surface of tissue. The surface heating that results from irradiation is different from the volumetric heating especially in situations of non-resonant absorption and unlike what happens in microwave ovens. In surface heating, the upper surface of substance/object is heated due to absorption of waves, which results in temperature rise. However, post absorption, the heat conducts to the volume, which lowers the peak temperature on skin. It is the peak temperature reached that is of interest in therapeutic effects. At higher frequency, the depth of penetration is very low, thus the surface of the tissue attains higher temperatures, and heating will occur at the surface of the tissue.

$$\nabla \times \mu_r^{-1} (\nabla \times \vec{E}) - k_0^2 \left( \epsilon_r \frac{j\sigma}{\omega - \epsilon_0} \right) \vec{E} = 0 \quad (1)$$

$$\nabla \times \mu_r^{-1} (\nabla \times \vec{E}) - k_0^2 \epsilon_r \vec{E} = 0 \quad (2)$$

$E$  is the electric field intensity,  $\mu_r$  the relative permeability,  $\epsilon_r$  the relative permittivity, and  $\sigma$  the conductivity. The above equations represent the wave propagation in the waveguide with time varying environment, where  $k_0 = 2\pi/\lambda_0$  is the wave number. Equation (1) can be rewritten for static condition, i.e., when conductivity ( $\sigma$ ) is zero, as represented in Equation (2). This boundary condition is applied during modeling of millimeter wave propagation through waveguide in COMSOL Multi-physics RF module.

$$n \times \vec{E} = 0 \quad (3)$$

The impedance boundary condition (IBC) is useful in the numerical technique which reduces the time required for the computation. This boundary condition is useful for calculating the scattering parameters of the of EM wave which is bombarded on the object [11]. The IBC will analyze only the surface of the object rather than the volume inside the object at high frequency shown in Equation (4).

$$\sqrt{\frac{\mu_0 \mu_r}{\epsilon_0 \epsilon_r - \left( \frac{j\sigma}{\omega} \right)}} n \times \vec{H} + \vec{E} - (n \cdot \vec{E}) n = (n \cdot \vec{E}_s) n - \vec{E}_s \quad (4)$$

The scattering parameter can be calculated using Equations (5) and (6). These equations give the ratio of integral impedance of reflected electric field in volts per meter.

$$\vec{S} = \frac{\int_0^4 (\vec{E} - \vec{E1}) \cdot \vec{E1}}{\int_0^4 \vec{E1} \cdot \vec{E1}} \quad (5)$$

$$\vec{S} = \frac{\int_0^4 \vec{E} \cdot \vec{E2}}{\int_0^4 \vec{E2} \cdot \vec{E2}} \quad (6)$$

The propagated wave should be scattered at the termination of the closed bounded structure in FEM. As perfect matched layer is created, the propagated wave is assumed to be scattered at that port [12]. The mathematical representation of this scattered wave boundary condition is given in Equation (7).

The tangential component of electric field decays along the  $r$  distance in meter. Equations (5) and (6) are in the closed boundary region  $0 < \partial\Omega < 4$  mm. The tangential component of electric field decays along the distance  $r$  in meter.

$$n \times (\nabla \times \vec{E}) - jkn \times (\vec{E} \times n) = -n \times (\vec{E}_0 \times (jk(n - k_{dir}))) e^{-jk_{dir}r} \quad (7)$$

Once the EM waves are incident on the object, it will produce heat in the solid [13]. The heat transfers in the solid are given in Equations (8) and (9).

$$\rho C_\rho \frac{\partial T}{\partial t} + \rho C_\rho \mu \cdot \nabla T + \nabla \cdot q = Q + Q_{ted} \quad (8)$$

where  $\rho$  is the density in kg/m<sup>3</sup>,  $C_\rho$  the specific heat capacity at constant pressure (J/kg·K),  $T$  the absolute temperature,  $u$  the velocity vector,  $q$  the heat flux by the conduction (W/m<sup>2</sup>),  $Q$  the heat sources other than viscous heating (W/m<sup>3</sup>), and  $Q_{ted}$  the initial heat of the tissue.

$$q = -k\nabla T \quad (9)$$

The heat insulation boundary condition is applied along the waveguide. The initial value of heat flux along the unit vector is null, given in Equation (10). This value increases with time to the saturation value of heat flux ( $q_0$ ) shown in Equation (11). These changes are opposed by the state hence the negative sign. This boundary condition is applied at the surface of the bent waveguide.

$$-n \cdot q = 0 \quad (10)$$

$$-n \cdot q = q_0 \quad (11)$$

Equation (8) can be replaced by Eq. (12) using Eq. (9)

$$\rho C_\rho \frac{\partial T}{\partial t} + \rho C_\rho \mu \cdot \nabla T = \nabla \cdot (k\nabla T) + Q_e \quad (12)$$

The equivalent heat source is the function of real and imaginary parts of electromagnetic waves described in Equations (13) to (15).

$$Q_e = Q_{rh} + Q_{ml} \quad (13)$$

$$Q_{rh} = \frac{1}{2} \text{Re} (J \cdot \vec{E}^*) \quad (14)$$

$$Q_{ml} = \frac{1}{2} \text{Re} (i\omega B \cdot \vec{H}^*) \quad (15)$$

The initial heat source on the boundary of waveguide is represented by  $Q_b$ . The total heat on the boundary ( $Q_b$ ) of waveguide is given in Equation (16).

$$-n \cdot (-k\Delta T) = Q_b \quad (16)$$

### 3. HEAT ANALYSIS ON TISSUE

It is observed that the heating of the object/substance because of microwave power is possible for the simple reason that millimeter wave possesses energy. The following equations describe the electromagnetic energy in terms of heat. The relationship between power density dissipated ( $P_{dis}$ ) in the material and the electric field intensity ( $E$ ) is given in Equation (17), where  $q_{abs}$  represents the heat generation term,  $\omega$  represents the angular frequency, and  $\epsilon''_{eff}$  is the complex imaginary permittivity of material. The complex permittivity combines with real part of permittivity ( $\epsilon'$ ) to give the material properties, i.e.,  $\epsilon = \epsilon' - j\epsilon''_{eff}$ .

$$P_{dis} = \omega \epsilon''_{eff} |\vec{E}|^2 = q_{abs} \quad (17)$$

$$\vec{E} = \vec{E}_0 e^{-\gamma z \bar{x}} \quad (18)$$

$$\vec{H} = \frac{\vec{E}_0}{\sqrt{\frac{\mu}{\epsilon}}} \cdot e^{-\gamma z} \cdot \bar{y} \quad (19)$$

The electromagnetic field has strong bounding component in terms of electric  $\vec{E}$  and magnetic field  $\vec{H}$  components with material permeability ( $\mu$ ) and material permittivity ( $\epsilon$ ) shown in Equations (18) and (19). In these equations,  $\gamma$  is the complex propagation constant along  $z$ -axis which is described in Equations (20) to (22) [8].

$$\gamma = \alpha + j\beta = \sqrt{j\omega\mu j\omega\epsilon} \tag{20}$$

$$\gamma = \omega\sqrt{\epsilon_0\mu_0}\sqrt{-\epsilon'_r + j\epsilon''_r} \tag{21}$$

$$\gamma = \frac{\pi(2\epsilon')^{1/2}}{\lambda_0} \left[ \sqrt{\left(1 + \left(\frac{\epsilon''_r}{\epsilon'_r}\right)^2\right)^{1/2}} - 1 + j\sqrt{\left(1 + \left(\frac{\epsilon''_r}{\epsilon'_r}\right)^2\right)^{1/2}} + 1 \right] \tag{22}$$

where relative dielectric constant is ( $\epsilon'_r = \epsilon'/\epsilon_0$ ), and relative loss factor is ( $\epsilon''_r = \epsilon''/\epsilon_0$ ), which are important factors and normalized with respect to free space permittivity ( $\epsilon_0$ ) which has direct relationship with wavelength  $\lambda_0$  given in Equation (23). Thus the electromagnetic fields can be rewritten as given in Equations (24) and (25).

$$\lambda_0 = \frac{2\pi}{\omega\sqrt{\epsilon_0\mu_0}} \tag{23}$$

The operating frequency for millimeter wave is 30 GHz, and wavelength is 1 cm. Thus the antenna has quarter wavelength for better radiation with maximum length 0.25 cm, i.e., 2.5 mm.

$$\vec{E} = \vec{E}_0 e^{\alpha z} e^{-j\beta z \bar{x}} \tag{24}$$

$$\vec{H} = \frac{\vec{E}_0}{\sqrt{\frac{\mu}{\epsilon}}} | e^{-\alpha z} e^{-j\beta z \bar{y}} \tag{25}$$

The power flux associated with propagating electromagnetic waves is given in Equation (26).

$$\vec{S} = \vec{E} \times \vec{H} = \frac{\sqrt{\epsilon}}{\mu} |\vec{E}_0|^2 e^{-2\alpha Z} \tag{26}$$

Thus, the power dissipated in the lossy material can be represented by Poynting vector as in the following Equations (27) and (28).

$$P_{dis} = -\text{Re}(\nabla \cdot \vec{S}) = \frac{2\alpha \text{Re}(\sqrt{\vec{E}^*})}{\sqrt{\mu}} |\vec{E}_0| e^{-2\alpha Z} \tag{27}$$

$$P_{dis} = \omega\epsilon''_r |\vec{E}_0| e^{-2\alpha Z} = q_{abs} \tag{28}$$

where  $E_0$  is the electric field component at  $z = 0$  the origin of the wave. The skin depth increases with wavelength, and its relationship is given in Eq. (29) [4]. The specific absorption rate (SAR) depends on the depth of penetration  $\delta$ , and they are the function of frequency. The relationship between SAR and depth of penetration is given in Equation (30) [6].

$$\delta = \frac{67.52}{f} \frac{1}{\sqrt{\sqrt{(\epsilon')^2 - (\epsilon'')^2} - (\epsilon')}} \tag{29}$$

$$\text{SAR} = \frac{2P_{in}(1 - |\rho|^2)}{\delta} \tag{30}$$

From Equations (29) and (30), the mathematical model of SAR can be represented as in Equation (31). This equation indicates that the SAR is directly proportional to the incident power ( $P_{in}$ ), frequency ( $f$ ), and power coupling coefficient ( $(1 - |\rho|^2)$ ).

$$\text{SAR} = 33.33fP_{in} (1 - |\rho|^2) \sqrt{\sqrt{(\epsilon')^2 - (\epsilon'')^2} - (\epsilon')} \tag{31}$$

The skin depth is 0.7 mm at 30 GHz frequency with input power 10 mW, and the power coupling coefficient is 0.5. This calculation is approximately matched with the experimentally calculated results by Alekseev et al. [14].

Now we can calculate SAR in terms of mass density.

From Equation (26) we obtain the incident power.

Incident power density =  $[(E^2)/377]$  from [1, 15]

From values considered in Section 2,

We can write incident power density =  $[E^2/377] = 0.66$

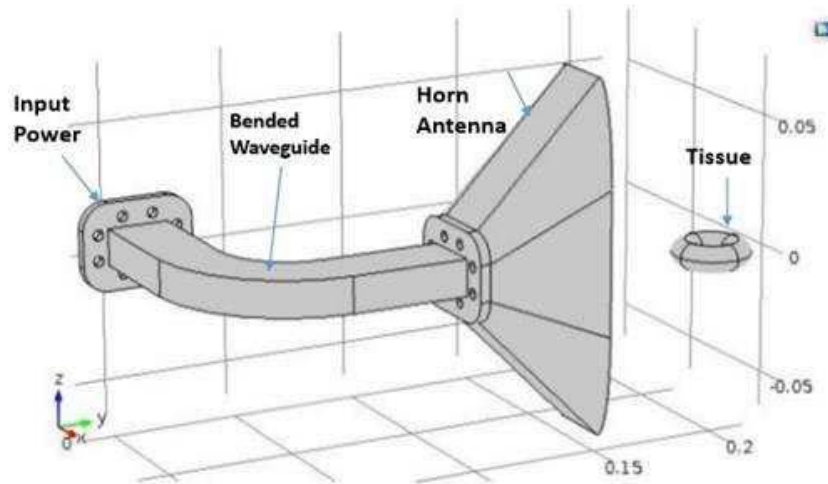
SAR =  $[[E^2]/Md]$  from [16]

SAR =  $[39.18 \times 25]/1100 = 0.89 \text{ W/kg}$

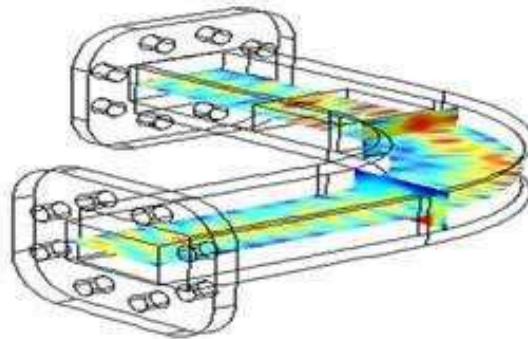
#### 4. ANALYSIS USING BEM AND FEM TECHNIQUES

Figure 3 shows the side view of the model to be simulated which is designed in COMSOL Multiphysics and depicts geometry of bent waveguide model extended with horn antenna and tissue placed in the free space. The MMW travels through the waveguide at 30 GHz as shown in Fig. 4. The millimeter wave gets detached from the waveguide and is launched into the free space shown in Figs. 5 and 6. The actual radiation of MMW wave on the tissue (placed in free space) takes place at the speed of wave, but thermalization takes more time.

The prolonged heating resulting in high temperature causes the damage of tissue. Thus, the interaction of MMW with the tissue is calculated in terms of variation of electric field intensity along the line. The line integral is calculated along the straight line from the point of source to tissue and



**Figure 3.** Side view of simulation model in COMSOL multiphysics.



**Figure 4.** Propagation of millimeter wave @30 GHz at 10 mW.

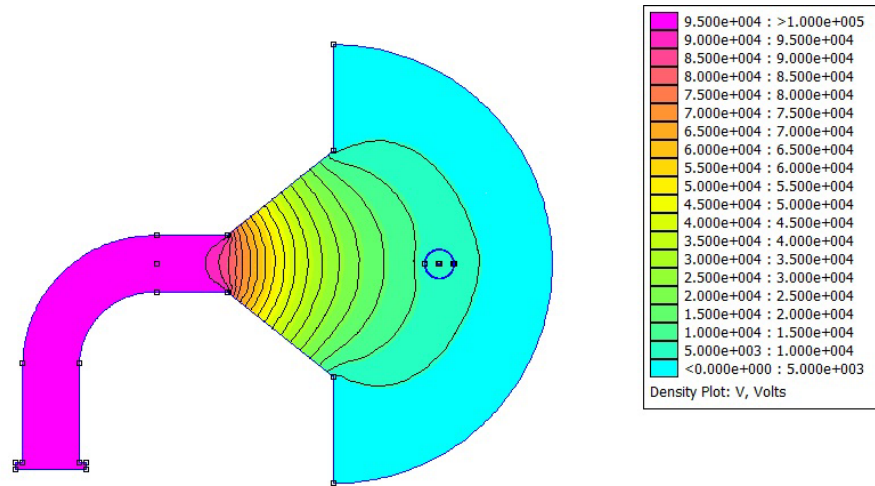


Figure 5. Potential variation and visualization of wave propagation.

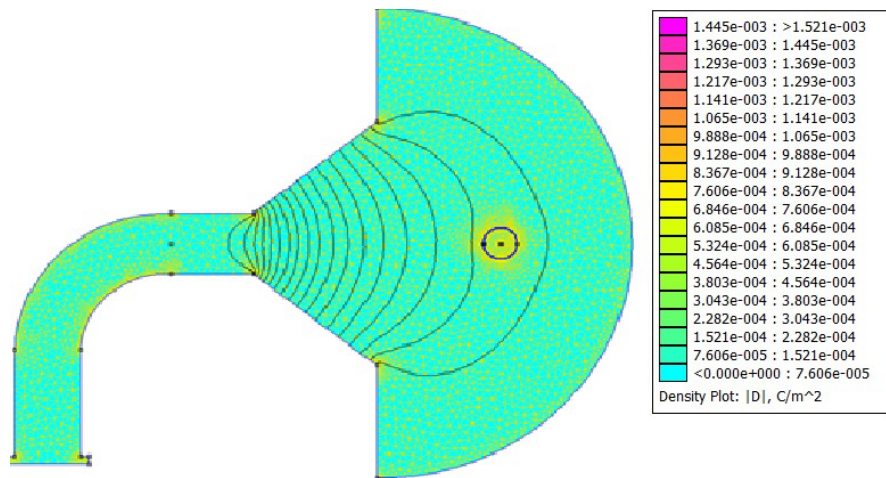


Figure 6. Variation of electric flux density ( $D$ ) within tissue.

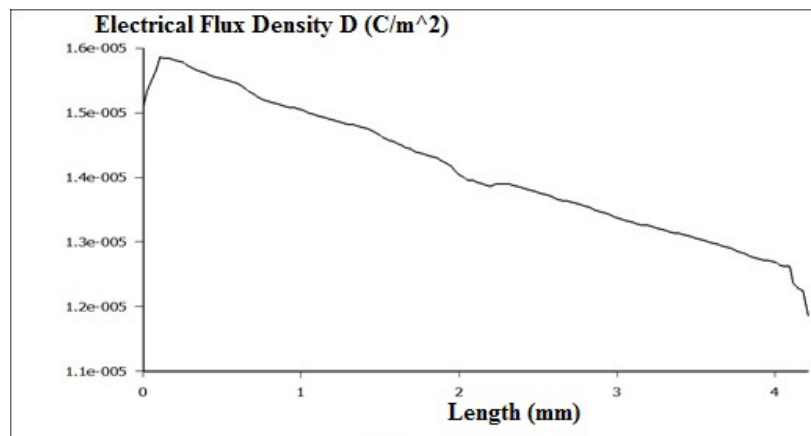


Figure 7. Variation of electric flux density ( $D$ ) within tissue.

within tissue. The detailed images are shown in Figs. 5 and 6. Thus, from this computation, we can get the effect of MMW on the tissue for various distances. In Fig. 5, potential variation is clearly visible due to the change in color whereas Fig. 6 shows the change in tissue temperature as electric flux density changes. Higher frequency causes more heating on the surface because the electric field intensity is higher on the surface, and it decreases with the depth of tissue which can be seen in plots 7 and 8. Thus, the depth of penetration is lower in the inner layer of the tissue than at outer layer at millimeter wave frequencies. Plot of variation of electric flux density (Fig. 7), as well as plot of electric field intensity (Fig. 8), shows that at higher frequency the penetration within the tissue goes on decreasing whereas it is higher in outer layer.

The reflection coefficient ( $S_{11}$ ) is  $-26$  dB at around 30 GHz, and the transmission coefficient ( $S_{21}$ ) approximately approaches zero at around same 30 GHz of operating frequency.  $S_{11}$  and  $S_{21}$  are shown in Fig. 9.  $S_{11}$  is quite good, so very low power is reflecting back, and radiated power is good. It indicates that power is transmitted from port 1 of waveguide to port 2 of the waveguide and then radiated on the tissue via horn antenna.

The tissue temperature variation versus time (sec) is shown in Fig. 10. The time is shown in terms of minutes in the upper right hand corner of plot, e.g., (0.25 min = 15 seconds shown on  $x$ -axis). The variation of temperature versus time is well developed, and it is modeled using network theory approach by Stewart et al. [7]. However, it is necessary to use the 3D modeling using field theory approach for

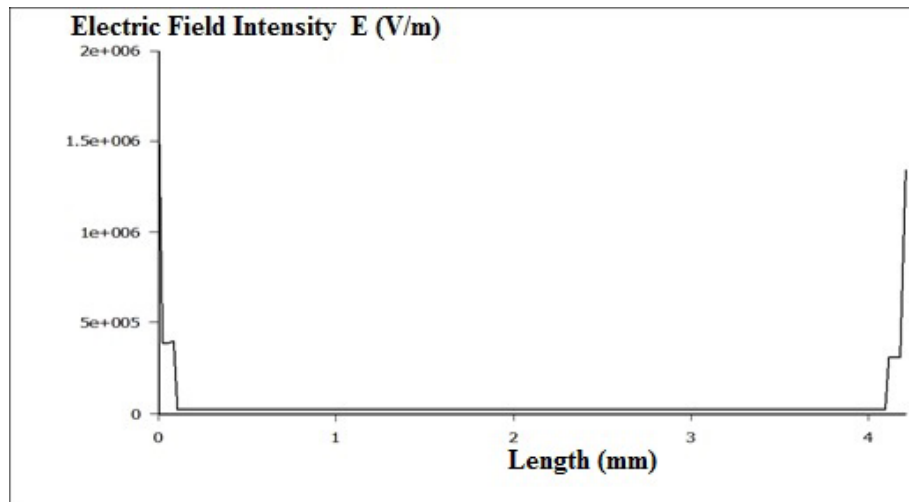


Figure 8. Variation of electric field intensity ( $E$ ) within tissue.

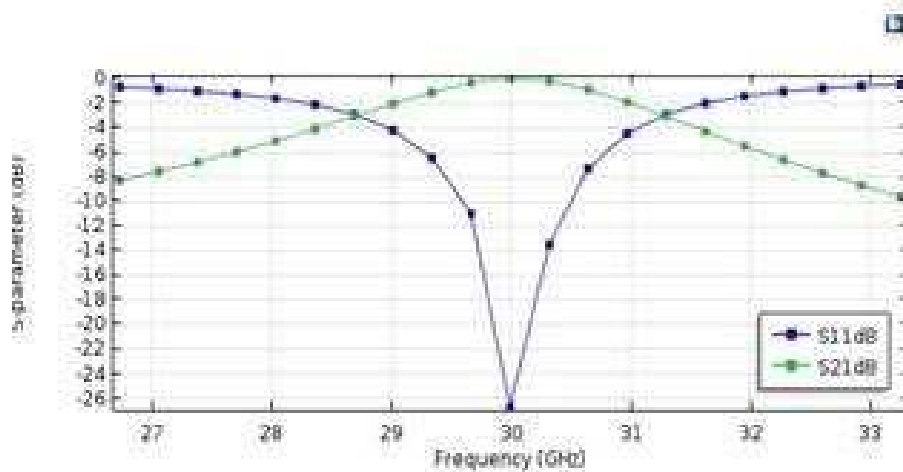
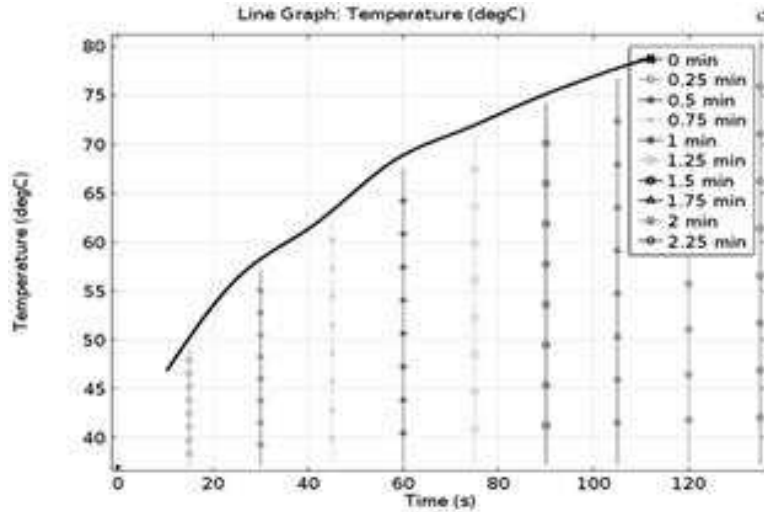


Figure 9.  $S_{11}$ -parameters variation.



**Figure 10.** Tissue temperature variation versus time (sec).

further development in higher frequency applications, and the results obtained by us show similar trends [Table 1] (also seen in work of others although frequencies and other details are different). Thus, with reference to our model, we reiterate that the temperature reached at the boundary of skin and inner layer reaches about 75 degrees, C, which is damaging as shown in Fig. 10.

**Table 1.** Comparison of temperature variation with time with the existing model.

Time (sec)	Temperature observed by Nelson et al. [4] in deg.Cel. at 100 GHz	Temperature observed by Stewart et al. [7] in deg.Cel. at 94 GHz	Temperature from modified model in deg.Cel. at 30 GHz
0	37	37	37
10	38.5	42	46
20	39.5	45	52
30	41	47	56
40	40	48	60
50	39	53	63
60	38.5	42	67

## 5. CONCLUSION

In this paper, the actual 3D visualization of millimeter wave propagation through bent waveguide to antenna for uniform exposure of three-layer biological tissue is modeled successfully. This is a novel way which the authors tried to implement via simulation and wanted to bring out some results with respect to tissue scales and thermal properties to show their relevance. From this proposed model, we analyze the SAR, depth of penetration, and *S*-parameters. As COMSOL Multiphysics is used, self-consistency between E/M and thermal effects is ensured without bothering calibrations. Hence, this model is helpful for the analysis of effects of MMW on tissue. It is observed that as the frequency increases, the radiation intensity increases with higher losses in the wave propagation. It is known that the biological tissue will experience permanent damage after 45 to 55-degree Celsius temperature and hence needs to be checked against other metabolic changes. More work on realistic approach to tissue damage considering its composition and also metabolic effects may be the focus of future work.

## ACKNOWLEDGMENT

We extend our gratitude towards our Principal, Ramrao Adik Institute of Technology, for his constant motivation and support.

## REFERENCES

1. Wu, T., T. S. Rappaport, and C. M. Collins, "The human body and millimeter-wave wireless communication systems: Interactions and implications," *2015 IEEE International Conference on Communications (ICC)*, 2423–2429, 2015.
2. Pely, A., K. R. Nightingale, and M. L. Palmeri, "Dispersion analysis in skin using FEM: Characterizing the effects of the lower boundary material on the propagation of shear waves," *IEEE International Ultrasonics Symposium Proceedings*, Tours, France, 2016.
3. Zilberti, L., D. Voyer, O. Bottauscio, M. Chiampi, and R. Scorretti, "Effect of tissue parameters on skin heating due to millimeter EM waves," *IEEE Transactions on Magnetics*, Vol. 51, No. 3, Mar. 2015.
4. Nelson, A., M. T. Nelson, T. J. Walters, and P. A. Mason, "Heating effects of millimeter-wave irradiation-thermal modeling results," *IEEE Transactions on Microwave Theory and Techniques*, Vol. 48, No. 11, 2111–2120, Nov. 2000.
5. Colombi, D., B. Thors, and C. Trnevik, "Implications of EMF exposure limits on output power levels for 5G devices above 6 GHz," *IEEE Antennas and Wireless Propagation Letters*, Vol. 14, 1247–1249, 2015.
6. Gandhi, O. P. and A. Riazi, "Absorption of millimeter waves by human being its biological implications," *IEEE Transactions on Microwave Theory and Techniques*, Vol. 34, No. 2, 228–235, Feb. 1986.
7. Stewart, D. A., T. R. Gowrishankar, and J. C. Weaver, "Skin heating and injury by prolonged mm wave exposure: Theory based on a skin model coupled to a whole body model and local biochemical release from cells," *IEEE Transactions on Plasma Science*, Vol. 34, No. 4, 1480–1493, Aug. 2006.
8. Pozar, D. M., *Microwave Engineering*, 4th Edition, Wiley and Sons Publication, 2012.
9. Vollmer, M., *Physics of Microwave Oven*, Physics Education, IOP Publishing Ltd, 2004.
10. Adhikari, P., *Understanding Millimeter Wave Wireless Communication*, White paper, Loea Corporation, 2008.
11. Mohsen, A., "On the impedance boundary condition," *Applied Mathematical Modelling*, Vol. 6, 405–407, Oct. 1982.
12. Li, W.-D. and W.-S. Dai, "Scattering theory without large-distance asymptotics: Scattering boundary condition," *Mathematical Physics*, Feb. 2015.
13. Pitchai, K., "Electromagnetics and heat transfer modelling of microwave heating in domestic ovens," Thesis, University of Nebraska, Lincoln, Nebraska, May 2011.
14. Alekseev, S. I., A. A. Radzievsky, M. K. Logani, and M. C. Ziskin, "Millimeter wave dosimetry of human skin," *Bioelectromagnetics*, Vol. 29, No. 1, 65–70, 2008.
15. Zhadobov, M., N. Chahat, R. Sauleau, C. L. Quement, and Y. L. Drean, "Millimeter wave interaction with the human body: State of knowledge and recent advances," *Int. Journal of Microwave and Wireless Technology*, 2011.